Supporting information for:

Submolecular Imaging by Noncontact Atomic Force Microscopy with an Oxygen Atom Rigidly Connected to a Metallic Probe

Harry Mönig,[*,†,‡] Diego R. Hermoso,[¶,||] Oscar Díaz Arado,[†,‡,||] Milica Todorović,[¶] Alexander Timmer,[†,‡] Simon Schüer,[†,‡] Gernot Langewisch,[†,‡] Rubén Pérez,[¶,§] and Harald Fuchs[†,‡]

Physikalisches Institut, Westfälische Wilhelms-Universität Münster, Wilhelm-Klemm-Strasse 10, 48149 Münster, Germany, Center for Nanotechnology (CeNTech), Heisenbergstrasse 11, 48149 Münster, Germany, Departamento de Física Teórica de la Materia Condensada, Universidad Autónoma de Madrid, 28049 Madrid, Spain, and Condensed Matter Physics Center (IFIMAC), Universidad Autónoma de Madrid, 28049 Madrid, Spain

E-mail: harry.moenig@uni-muenster.de

---

[*] To whom correspondence should be addressed

[†] Westfälische Wilhelms-Universität Münster

[‡] Center for Nanotechnology (CeNTech)

[¶] Universidad Autónoma de Madrid

[§] Universidad Autónoma de Madrid II

[||] These authors contributed equally to this work.

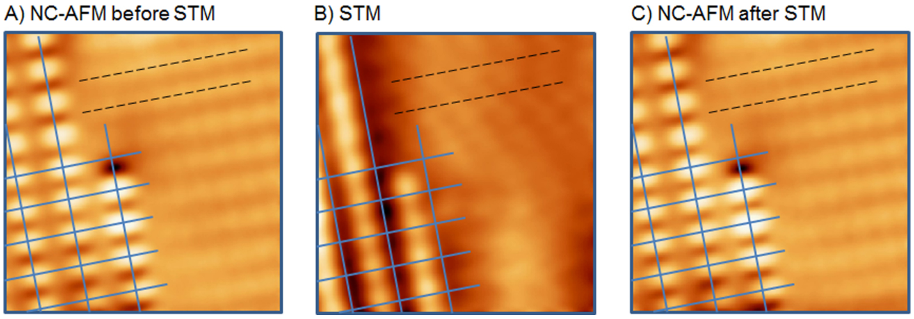

Figure S1: Sequence of consecutively recorded images $(3 \times 3\text{nm}^2)$ showing that lateral drift can be excluded as origin of the pronounced shift of the maxima in the NC-AFM and STM channels. (A) NC-AFM image from Figure 1C (main manuscript). (B) STM image from Figure 1D (main manuscript). (C) NC-AFM image with the same imaging settings as used in A, recorded directly after the STM image in B. Imaging parameters NC-AFM: $\Delta f = -6.0\text{Hz}$; bias voltage $U_{\text{gap}} = 0.0\text{V}$ (A and C); STM: current set-point $I = 0.5\text{nA}$; $U_{\text{gap}} = 0.1\text{V}$ (B).

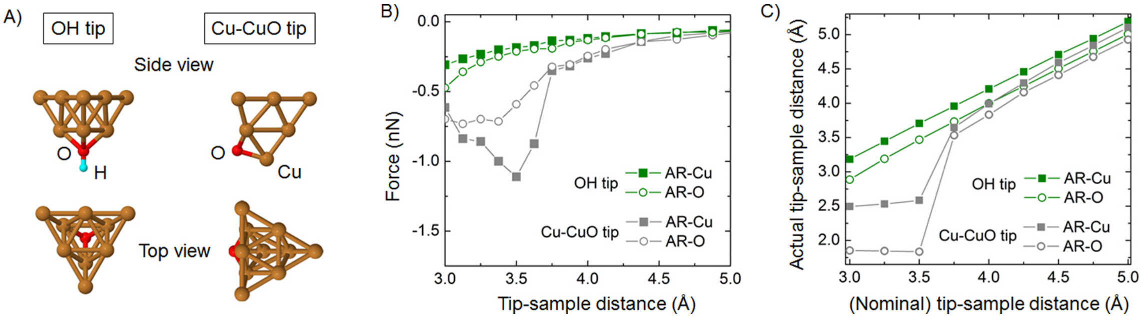

Figure S2: (A) Additional model tips considered as candidates to describe the experimental force contrast in Figure 2 (main manuscript). (B) Corresponding force-distance curves and, (C) nominal versus actual tip-sample distance showing similar relaxations as observed for the Cu and CuO tips. B and C are plotted with the same scales as the data presented in Figure 2H and 2J, respectively.

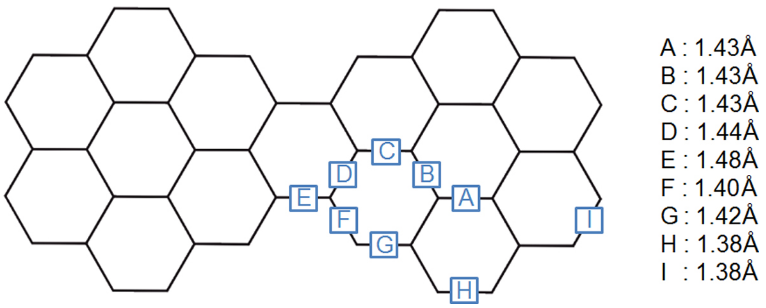

Figure S3: Theoretically determined bond lengths for the a DCLN molecule in the gas phase.

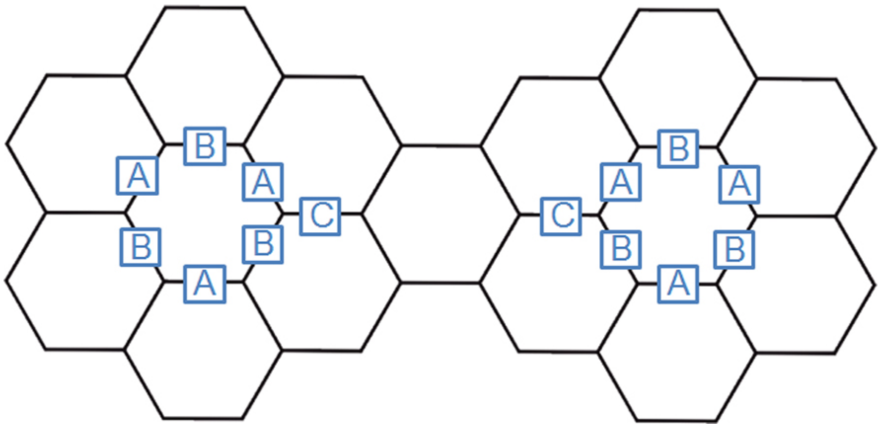

	Bonds A	**Bonds B**	**Bonds C**	**Mean value**
Experiment	1.50 ± 0.25	1.41 ± 0.27	1.42 ± 0.08	1.45 ± 0.23
DFT	1.43	1.43	1.43	1.43

Figure S4: Comparison of experimentally and theoretically determined bond lengths. Due to the increased Δf contrast of the outer bonds, only the inner bonds were considered. All values are given in angstrom.

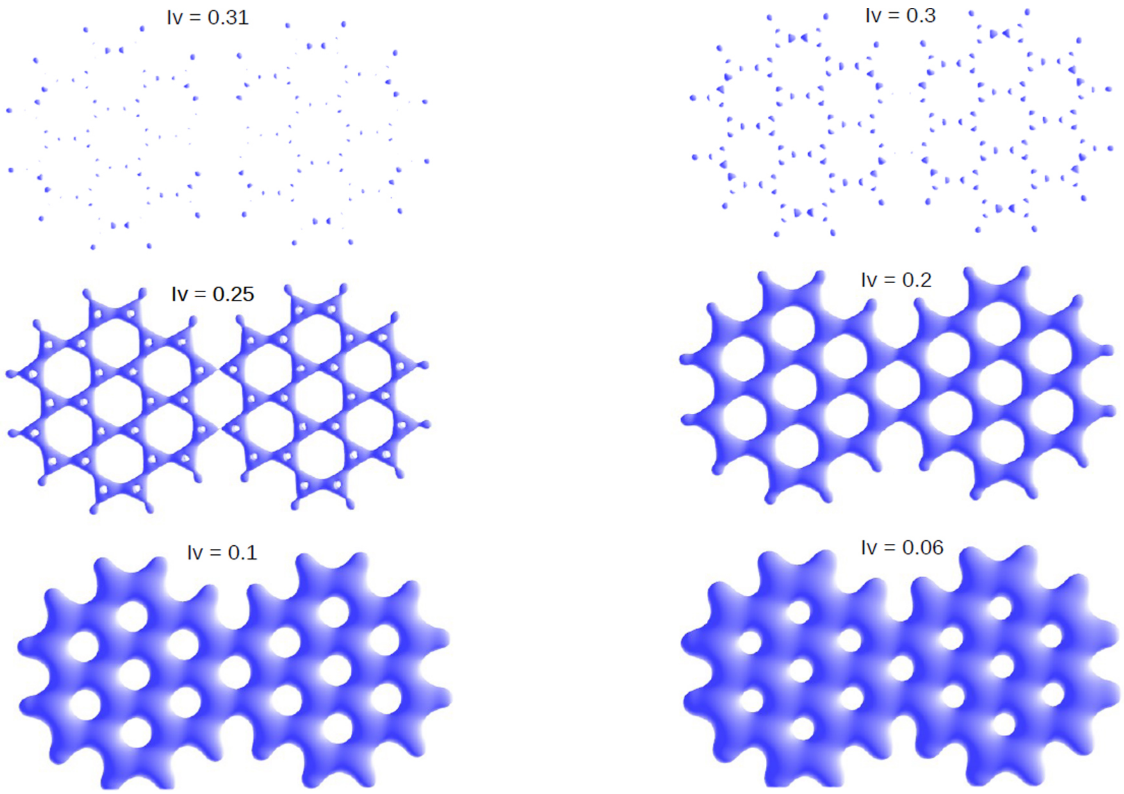

Figure S5: Theoretically determined total charge densities of dicoronylene (DCLN) for different isosurfaces. At isovalues $I_v = 0.31$ and 0.30, an increased charge density at the outer bonds can be seen. It is accompanied by a slight reduction in lengths of these bonds as shown in Figure S3.

Table S1: Elemental electronegativities of atoms that terminate various tips, which produce image contrast with intramolecular resolution in NC-AFM. Despite its relatively low electronegativity, Xe functionalized tips show good performance in submolecular imaging. In this case the reason is probably the high polarizability of xenon supporting an inhomogeneous charge distribution at the apex. All values are taken from Furtado *et al.*[S1]

Tips	Tip termination	Elemental electronegativity (eV)
CO	O	7.89
NTCDI[a]	O	7.89
CuO[b]	O	7.89
Cl	Cl	8.34
Br	Br	7.78
Xe	Xe	5.34

[a] Naphthalene tetracarboxylic diimide.

[b] O-terminated Cu tip (present work).

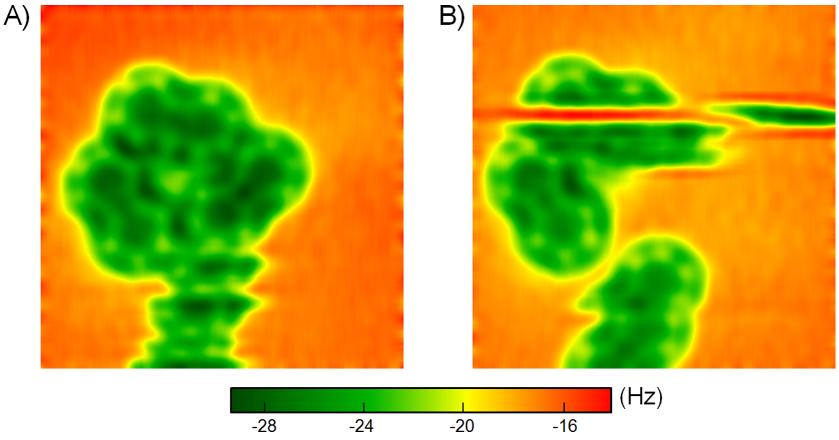

Figure S6: $5.5 \times 5.5\text{nm}^2$ constant height NC-AFM images of an assembly of three DCLN molecules adsorbed on an oxygen-induced $(2\sqrt{2} \times \sqrt{2})\text{R}45^\circ$ missing row reconstruction on Cu(100). Both images were consecutively recorded at the same tip-sample distance showing the lateral displacement of the molecules during scanning. Although the images are recorded in the attractive regime, the structure of the outer bonds is clearly visible.

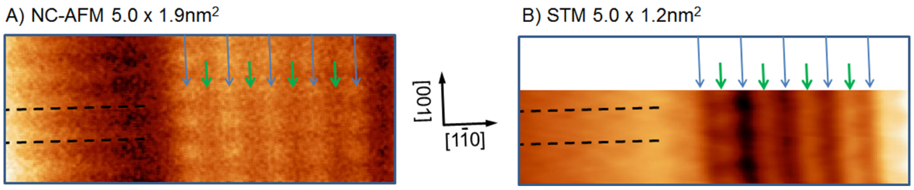

Figure S7: NC-AFM and STM images recorded on the same site prior the constant height measurement on DCLN (Figure 4B) to verify an O-termination in this experiment. Analog to the data in Figure 1 (main manuscript), first the NC-AFM image (A) was recorded ($\Delta f = -8.2\text{Hz}$, $U_{\text{gap}} = 0.0\text{V}$) and subsequently the STM image without qPlus oscillation (B) ($U_{\text{gap}} = 0.1\text{V}$, $I = 0.5\text{nA}$). Similar to Figure 1C and 1D, the position of the black dashed lines mark the Cu rows along the $[1\bar{1}0]$ direction. This shows that the maxima within the added rows can be assigned to the position of the Cu atoms. The five added rows along $[001]$ as imaged by NC-AFM are marked by blue arrows. Green arrows indicate the position of the four maxima as imaged by STM. Besides imaging Cu atoms in the oxide domain, the STM maxima located in between the added rows allow to conclude on an O-terminated tip apex.

References

(S1) Furtado, J.; Proft, F. D.; Geerlings, P. The Noble Gases: How Their Electronegativity and Hardness Determines Their Chemistry. *J. Phys. Chem. A* **2015**, *119*, 1339–1346.